Supplementary Information

Bottom-up Synthesis of High-performance Nitrogen-enriched Transition Metal/ Graphene Oxygen Reduction Electrocatalysts both in Alkaline and Acid Solution

Qingxue Lai, [a] Qingwen Gao, [a] Qi Su, [a] Yanyu Liang,* [a] Yuxi Wang,[b] and Zhi Yang*[b]

[a]College of Material Science and Technology, Nanjing University of Aeronautics and Astronautics

Yudao St. 29, 210016, Nanjing, P. R. China

[b]Key Laboratory for Thin Film and Microfabrication of Ministry of Education,Shanghai Jiao Tong University

Dongchuan Road 800, 200240, Shanghai, P. R. China

E-mail: liangyy403@126.com (Y.Y. Liang)

zhiyang@sjtu.edu.cn (Z. Yang)

Materials and Methods

1. Chemicals and Materials

FePc ($C_{32}H_{16}FeN_8$, TCI, >90%), CoPc ($C_{32}H_{16}CoN_8$, TCI, >90%), NiPc ($C_{32}H_{16}NiN_8$, J&K Chemical, >95%), Melamine ($C_3H_6N_6$, J&K Chemical, 99%), Concentrated sulfuric acid (H_2SO_4, 95%-98%, Nanjing Chemical Reagent Co., Ltd). All reagents were used as received without further purification.

2. Materials Synthesis

In a typical procedure, 4.000 g melamine and 60mg TMPc (TM=Fe, Co, Ni) were mixed together by grinding to form a uniform white mixture. Heat treatment of the mixture was placed in a crucible with a lid and treated in a tubular furnace under N_2 atmosphere at 600°C for 3 h, followed by annealing at 900°C for 1 h. Subsequently, the furnace was cooled to room temperature slowly and N-TM/G (60)-900 catalyst was obtained without other treatment. In order to get stable catalysts applied in acid solution, the abtained catalysts were further treated with 2M H_2SO_4 at 80°C for 8 hours follwed by second heat treatment at the same temperature under N_2 atmosphere and N-TM/G (60)-900-S catalysts were obtained. Different catalysts with controllabe structure and composition properties were also prepared by facilly regulating the synthesis conditions, for example, the addtion of TMPc and the heat treatment temperature.

3. Materials Physical Characterizations

The composition was examined by XRD (Rigaku Corporation D/max-2200/PC). The Raman spectra were obtained on Bruker Optics, Senterra R200-L (Germany) with excitation by an argon ion laser (532 nm). The morphology and microstructure were investigated by TEM (Philips Tecnai 12), HRTEM (Philips Tecnai G2), STEM (FEI Tecnai G2 F30 S-TWIN). The surface elemental composition was determined by XPS (Kratos AXIS Ultra) measurements. The porous structure were measured with a Micrometrics ASAP2020 analyzer (USA) at 77 K. TG-DSC was tested on NETZSCH STA 409TG (Germany) with a heat rate of 10°C/min under O_2. Mössbauer spectra were recorded at room temperature in the transmission mode using MS 500 (Oxford Instruments, U.K.) with a ^{57}Co/Pd-source, and the calibration is made with respect to α-Fe.

4. Electrochemical Measurements

1.0 mg prepared catalyst or commercial 30 wt% Pt/C catalyst was dispersed in 1.00 mL 0.05wt% Nafion ethanol solution and sonicated for about 45 minutes to form a homogeneous ink solution. Electrochemical measurements were conducted using a three-electrode cell with SCE (saturated calomel electrode) and platinum sheet were used as the reference and counter electrodes, respectively. ORR tests were carried out in O_2 or N_2-saturated 0.1M KOH or 0.1M $HClO_4$ electrolyte at room temperature on a CHI760D electrochemical workstation assembled with MSR Electrode Rotator (Pine Research Instrumentation). The test potential was transferred with respect to reversible hydrogen electrode (RHE) based on the equations: E (RHE) = E (SCE) +0.990V (in 0.1M KOH) and E (RHE) = E (SCE) +0.303V (in 0.1M $HClO_4$). The four-electron selectivity of catalysts was evaluated based on the HO_2^- or H_2O_2 yield and electron transfer number (n), calculated from the following equations:

$$H_2O_2 \text{ (or } HO_2^-)(\%) = 200 \times \frac{I_R/N}{I_R/N + I_D} \quad (1)$$

$$n = 4 \times \frac{I_D}{I_R/N + I_D} \quad (2)$$

Here, I_D and I_R is the disk and ring current, respectively, and N is the ring collection efficiency (0.37).

In addition, considering that high catalyst loading leads to high current background during the LSV test in acid solution, background deduction is performed via subtract the current response in N_2-saturated solution from the response in O_2-saturated solution at the same rotation of 1600 rpm.

Figure S Captions

Table S1. Several surface characteristics of prepared N-Fe/G materials. (Peak pore size and average pore size in BJH adsorption pore size distribution)

Table S2. Mössbauer parameters for the fitted lines for various samples.

Figure S1. TG/DSC curves of N-TM/G (60)-900 in air: (a) N-Fe/G (60)-900; (b) N-Fe/G (60)-900; (c) N-Fe/G (60)-900. The residual relative mass is 30.66%, 32.07% and 32.15%, respectively. Therefore the relative mass of metal in the corresponding catalyst is 21.44%, 23.55% and 25.26%, respectively.

Figure S2. Magnetic hysteresis loops of of N-TM/G. The saturation magnetization value is 15.9 emu/g, 14.2 emu/g and 2.4 emu/g for N-Fe/G (60)-900, N-Co/G (60)-900 and N-Ni/G (60)-900, respectively. (The weight used here is the total weight of the prepared catalyst)

Figure S3. (a) XRD pattern of the intermate product pyrolyzed of the mixture of melamine and FePc at 600^{o}C; (b-d) TEM images of the intermate product.

Figure S4. High-resolution XPS spectra of the intermate product pyrolyzed of the mixture of melamine and FePc at 600^{o}C.

Figure S5. N_2 adsorption−desorption isotherms (a, c) and BJH adsorption pore size distribution curves (b, d).

Figure S6. TEM images of N-Fe/G (60)-T and corresponding size contribution of Fe_3C NPs: (a, d, g) 800; (b, e, h) 900; (c, f, i) 1000.

Figure S7. Mössbauer spectra of the prepared N-Fe/G (60)-900 catalyst. A typical Fe^{2+}-N_4/C (D1) sites with a percentage of 15.5% are observed in this catalyst.

Figure S8. RRDE curves (a) and the electron transfer number (n) of the N-TM/G hybrids and 30% Pt/C at various potentials based on the corresponding RRDE data in (a).

Figure S9. CV (a), RDE (b), RRDE (c) and electron transfer number (n) of N-Fe/G (W)-900 at various potentials based on the corresponding RRDE data in (c).

Figure S10. CV (a), RDE (b), RRDE (c) and electron transfer number (n) of N-Fe/G (60)-T at various potentials based on the corresponding RRDE data in (

Table S1

Samples	Surface area (m^2/g)	Pore volume (m^3/g)	Peak pore size (nm)	Average pore size (nm)
N-Fe/G(60)-800	342.6	0.999	3.71	23.7
N-Fe/G(60)-900	404.5	1.156	3.73	17.3
N-Fe/G(60)-1000	434.8	1.299	3.69	17.0
N-Fe/G(200)-900	182.5	0.432	3.81	19.3
N-Fe/G(100)-900	322.6	0.764	3.83	18.4
N-Fe /G(30)-900	622.3	1.769	3.64	16.9

Table S2

Sample	Peak	δ(mm/s)	ΔE_Q(mm/s)	H_{hf} (KOe)	FWHM(mm/s)	Area Ratio(%)
N-Fe/G(60)-900	Sing	0			0.19	5.6
	D1	0.34±0.03	1.21±0.06		0.75±0.02	15.5
	Sext1	0.29±0	-0.02±0	210.2±0.3	0.31±0	51.9
	Sext2	0.01±0.04	0	334.7±2	0.93±0.02	26.9
N-Fe/G(60)-800-S	Sing	0.12±0.01			0.40±0.01	6.8
	D1	0.50±0.01	1.31±0.01		0.40±0.01	26.6
	D2	0.59±0.01	2.26±0.02		0.54±0	25.4
	D3	0.89±0.01	3.59±0.03		0.37±0.01	8.8
	D4	1.00±0	2.64±0.04		0.67±0.01	19.3
	Sext1	0.30±0.01	-0.06±0.03	216.6±1	0.20±0.02	7.0
	Sext2	0.01±0.04	0	332.0±1	0.23±0.02	6.01
N-Fe/G(60)-900-S	Sing	-0.01±0.01			0.20±0.01	7.2
	D1	0.31±0.04	0.69±0.07		0.47±0.03	9.8
	D3	0.39±0.09	2.97±0.1		1.31±0.06	21.7
	Sext1	0.29±0	-0.03±0.01	213.6±0.6	0.30±0	36.6
	Sext2	0.05±0.08	-0.12±0.1	319.8±5	0.93±0.04	24.7
N-Fe/G(60)-1000-S	Sing	-0.02±0.01			0.30±0.01	6.4
	D1	0.44±0.02	0.87±0.04		0.26±0.01	5.8
	Sext1	0.29±0	0.02±0	210.7±0.1	0.20±0	64.1
	Sext2	0.09±0	0.02±0.01	332.8±0.4	0.19±0	23.7

Figure S1

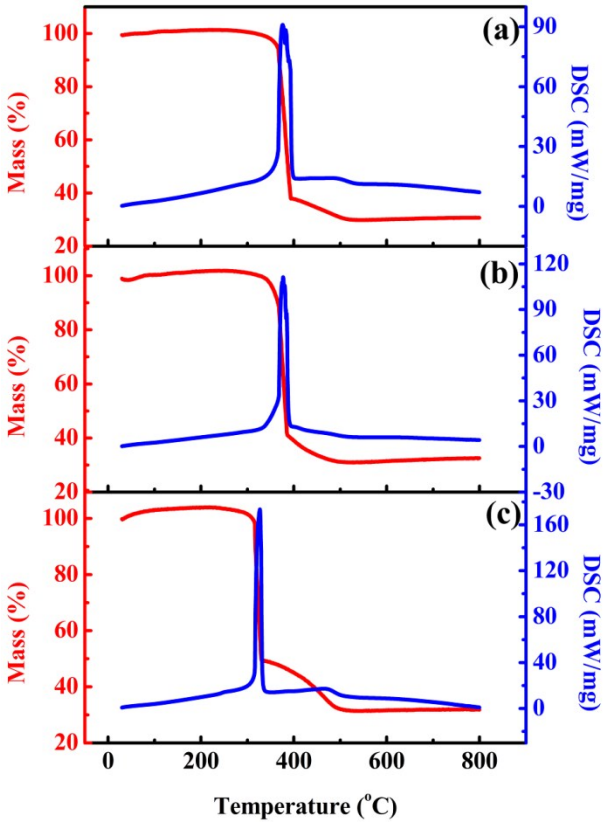

Figure S2

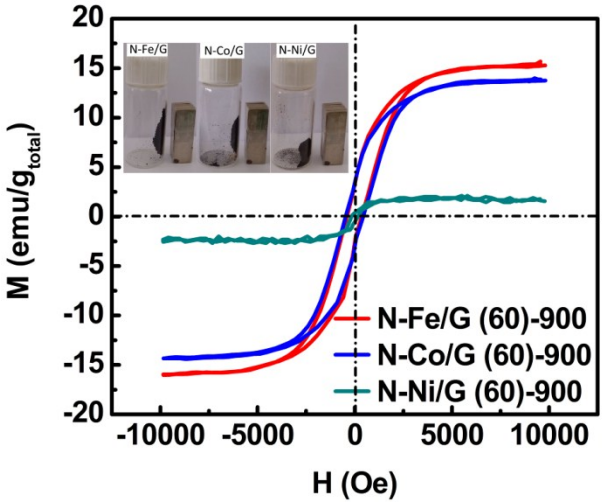

Figure S3

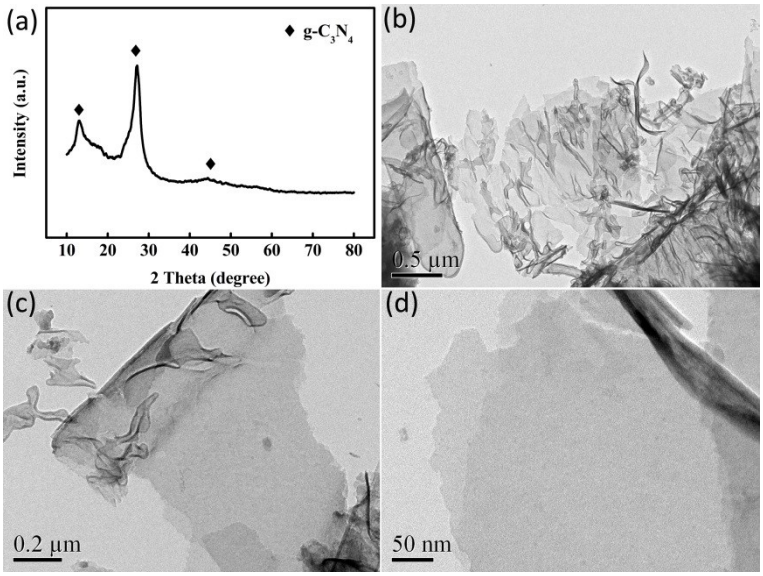

Figure S4

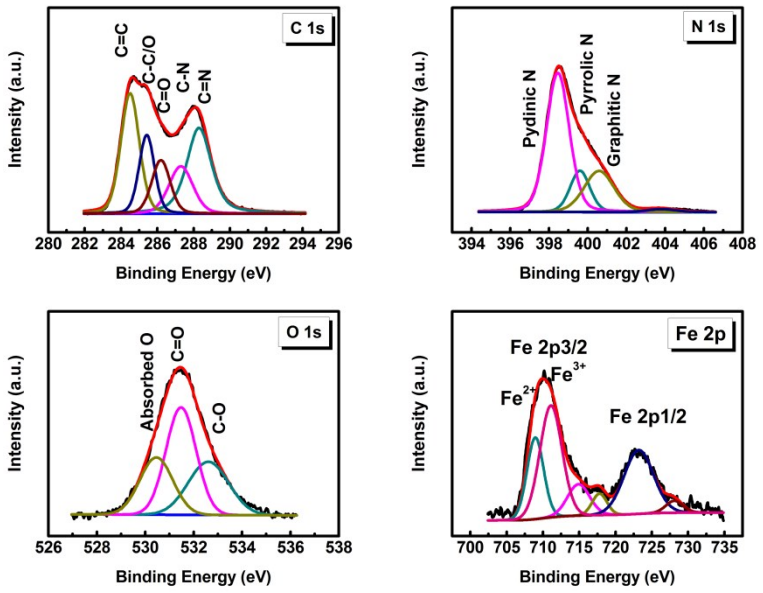

Figure S5

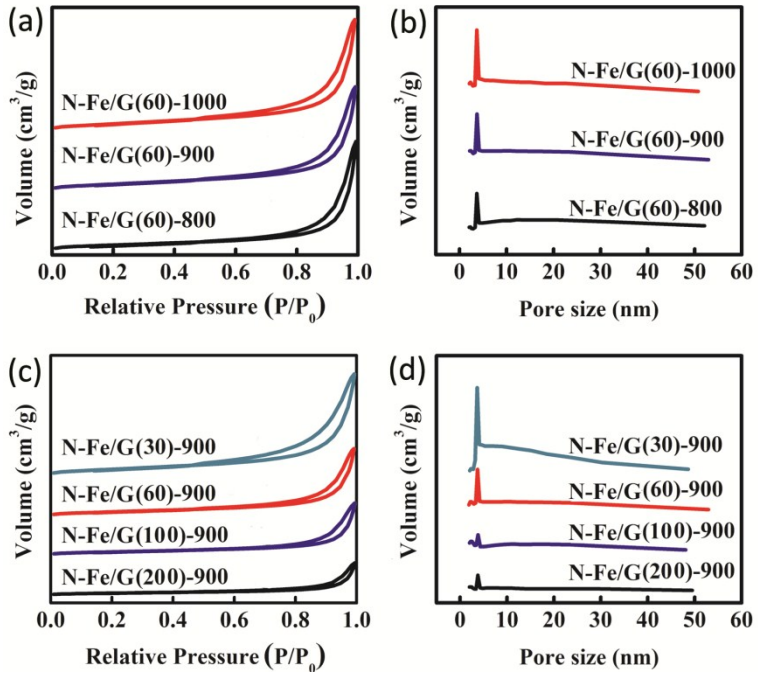

Figure S6

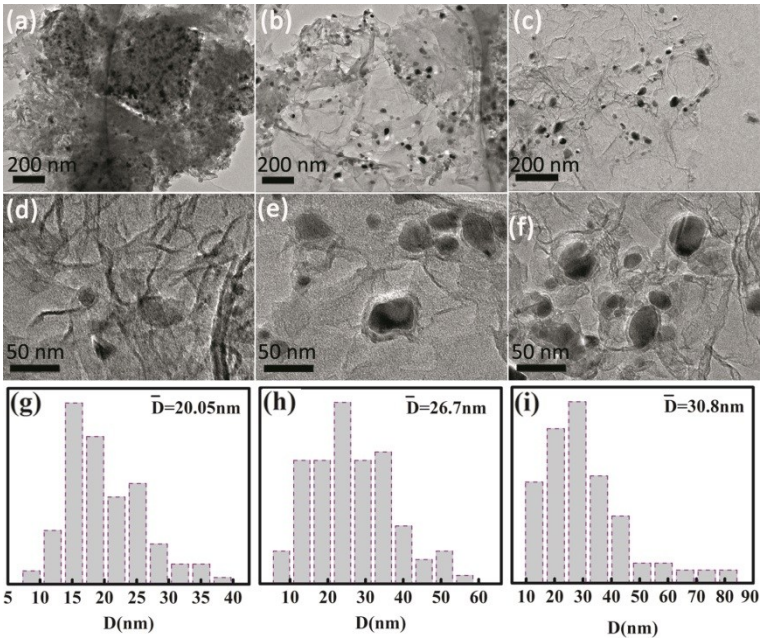

Figure S7

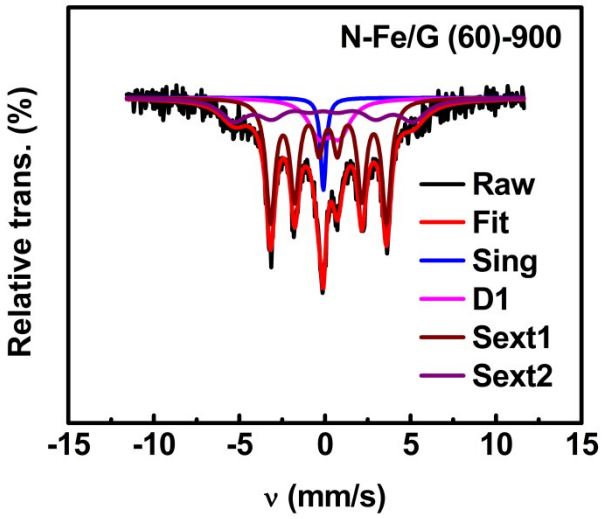

Figure S8

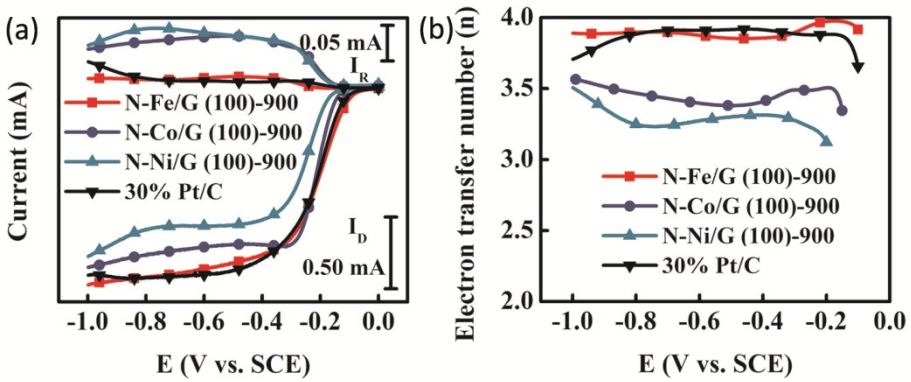

Figure S9

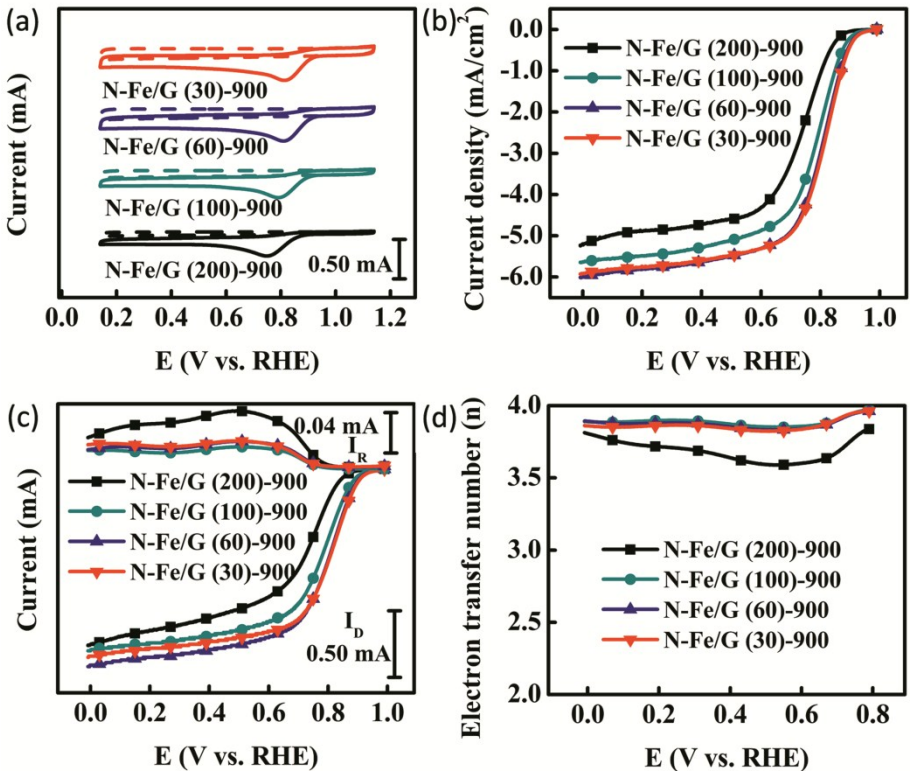

Figure S10